ISSN 0010-5082, Combustion, Explosion, and Shock Waves, 2018, Vol. 54, No. 6, pp. 629–641. © Pleiades Publishing, Ltd., 2018.
Original Russian Text © M.A. Goldfeld, Yu.V. Zakharova, A.V. Fedorov, N.N. Fedorova.

Effect of the Wave Structure of the Flow in a Supersonic Combustor on Ignition and Flame Stabilization

M. A. Goldfeld[a], Yu. V. Zakharova[a], A. V. Fedorov[†a], and N. N. Fedorova[a,b]

UDC 621.452:51-72

Published in *Fizika Goreniya i Vzryva*, Vol. 54, No. 6, pp. 3–16, November–December, 2018.
Original article submitted July 28, 2017.

Abstract: Results of numerical and experimental investigations of a high-velocity flow in a plane channel with sudden expansion in the form of a backward-facing step, which is used for flame stabilization in a supersonic flow, are presented. The experiments are performed in the IT-302M high-enthalpy short-duration wind tunnel under the following test conditions: Mach number at the combustor entrance 2.8, Reynolds number $30 \cdot 10^6$ m^{-1}, and total temperature $T_0 = 2000$ K, i.e., close to flight conditions at M = 6. The numerical simulations are performed by solving full unsteady Reynolds-averaged Navier–Stokes equations supplemented with the k–ω SST turbulence model and a system of chemical kinetics including 38 forward and backward reactions of combustion of a hydrogen–air mixture. Three configurations of the backward-facing step are considered: straight step without preliminary actions on the flow, with preliminary compression, and with preliminary expansion of the flow. It is demonstrated that the backward-facing step configuration exerts a significant effect on the separation region size, pressure distribution, and temperature in the channel behind the step, which are the parameters determining self-ignition of the mixture. The computed results show that preliminary compression of the flow creates conditions for effective ignition of the mixture. As a result, it is possible to obtain ignition of a premixed hydrogen–air mixture and its stable combustion over the entire channel height.

Keywords: supersonic flow, turbulence, shock wave, expansion wave, combustor, premixed mixture, ignition.

DOI: 10.1134/S0010508218060011

INTRODUCTION

The backward-facing step is one of the most popular geometric configurations used to study flying vehicles and their elements. The flows past the forward-facing step and the backward-facing step are considered as important examples of separated flows. The physical mechanism of separation in a supersonic flow past a backward-facing step is rather complicated and requires careful investigations. There are many experimental and numerical studies in this field (see, e.g., [1–4]).

The backward-facing step configuration is used in various applications, first of all, as an element of the rear part of the body, which affects the base pressure and reduces the drag of flying vehicles designed for various purposes [4]. The interest to the flow past a backward-facing step has recently revived owing to studies of supersonic combustors [5].

The main goal of the study in [6] was to determine the possibility of increasing the base pressure by means of changing the trailing edge shape. Significant efforts in previous years were focused on incompressible flows [7, 8]. Experimental investigations of laminar, transitional, and turbulent separated flows in the vicinity of a two-dimensional backward-facing step were performed in [7]. Detailed information on the flow structure and separation zone length in a wide range of Reynolds numbers was presented. It was demonstrated

[†]Deceased.

[a]Khristianovich Institute of Theoretical and Applied Mechanics, Siberian Branch, Russian Academy of Sciences, Novosibirsk, 630090 Russia; nfed@itam.nsc.ru.
[b]Novosibirsk State University of Architecture and Civil Engineering (SIBSTRIN), Novosibirsk, 630008 Russia.

that the separation zone length in a laminar flow increases with increasing Reynolds number, but this increase is not a linear function as in axisymmetric flows with sudden expansion. This effect was observed up to Reynolds numbers corresponding to the transitional flow regime.

Numerical simulations of flows in channels with backward-facing steps were performed in [8, 9], where a possibility of correct prediction of flow parameters and separation zone sizes was demonstrated. However, these data were obtained for low velocities of the flow and cannot be used for supersonic flows where the effects of compressibility are important. Supersonic flows in the base region of missiles and rockets were considered in [10, 11]. It was found that a correct choice of the shape of the base part of the body allows considerable reduction of the base drag [10].

The experimental and numerical data [11, 12] significantly contribute to understanding of the specific features of separated flows and to estimating the efficiency of various numerical methods.

Parker-Lamb and Oberkampf [13] provided a detailed review of experimental investigations of the base pressure and heat transfer for supersonic ad hypersonic flow velocities. The results obtained show that a supersonic flow behind a backward-facing step is characterized by a high level of nonuniformity and includes rapid expansion on the sharp edge of the step, separation, and reattachment of the boundary layer with the formation of an extended region of the flow with a positive (adverse) pressure gradient. The flow is characterized by an increase in the Mach number of the external flow, nonzero angle of the local flow, and variable pressure gradient in the entire domain behind the step.

Empirical relations were developed for estimating the base pressure and heat transfer in plane and axisymmetric configurations. These relations are applicable in wide ranges of Mach and Reynolds numbers for laminar and turbulent flows. A comparison of flight data and wind tunnel test results revealed that the derived relations can be used for predicting the flow parameters.

The state of the boundary layer ahead of the step is an important factor affecting the flow parameters behind the step and the base pressure level. Based on the generalization of available experimental and numerical data, Aukin and Tagirov [14] developed an approximate method of calculating the base pressure and enthalpy in supersonic flows behind plane and axisymmetric steps. The method is based on using the model of viscous-inviscid interaction and allows one to determine the base flow parameters for arbitrary thicknesses of the initial boundary layer for free-stream Mach numbers from 1 to 6. The model takes into account the existence of an extended region of increasing pressure in the separation zone behind the step and the special condition of flow reattachment.

It was demonstrated [15–17] that rapid expansion of the flow behind the step can significantly distort the mean characteristics and structure of the turbulent boundary layer, which exerts a pronounced effect on the specific features of flow separation, shear layer growth rate, and flow reattachment [6, 17]. It was found that the pressure and heat fluxes increased along the channel wall and their distributions depend on the step height and shape. It was also demonstrated that sudden expansion of the channel decreases the level of turbulence in a compressible boundary layer.

Numerical simulations of the flow in the vicinity of the backward-facing step is usually based on solving the Reynolds-averaged Navier–Stokes (RANS) equations. Correa and Warren [18] used the explicit MacCormack scheme and the k–ε turbulence model for a numerical analysis of sudden expansion of a supersonic flow. Yang et al. [19] performed a detailed theoretical study of the supersonic flow structure in the vicinity of a backward-facing step with the use of the LU-SSOR flux vector splitting for solving the governing equations and the algebraic Baldwin–Lomax model of eddy viscosity. Comparisons of numerical and experimental data revealed their good agreement.

A supersonic turbulent flow past a backward-facing step was numerically simulated in [20] with the use of the finite volume method and k–ε turbulence model. It was demonstrated that the method can predict all essential features of the flow and ensures reasonable agreement of numerical and experimental results. Liu et al. [5] simulated a supersonic flow past a step with the use of the RANS approach and Large Eddy Simulation (LES) technique. The influence of the Mach number ahead of the step and the degree of channel expansion was also studied. It was shown that the separation zone length decreases with increasing Mach number and the step height exerts a significant effect on the flow structure. The numerical and experimental data were found to be in good agreement. The data [5] are useful for understanding the physical nature of supersonic flow separation, but the authors did not consider the influence of the step shape and boundary layer state upstream of the separation point on the channel flow structure.

At the moment, much attention is paid to studying large-scale vortex structures developed in the mixing layer above the separation zone and playing a key role in mass, momentum, and energy transfer between the recirculation zone and external inviscid flow [21]. The capabilities of traditional turbulence models based on the RANS approach in resolving the spectrum of vortices

shed from the backward-facing step edge are rather limited. Implementation of vortex-resolving approaches, such as LES or DES (hybrid RANS–LES method) is the necessary condition for obtaining a full spectrum of vortices [22], but significant computer resources are needed for this purpose.

The analysis shows that it is necessary to use appropriate turbulence models and high-order numerical schemes for obtaining detailed information on the flow structure and reaching good agreement of experimental and numerical data.

In ramjet/scramjet technologies, the backward-facing step is considered as a flame holder in a supersonic combustor [23–25]. The flow behind the backward-facing step is characterized by the presence of a low-velocity recirculation zone, which increases the residence time of the mixture in the high-temperature region and forms a continuous source of mixture self-ignition [26]. Huang et al. [27] considered the mechanisms of flame stabilization in a supersonic combustor with the use of a backward-facing step and a cavity. It was demonstrated that vortices formed in the recirculation zone assist in mixing of the fuel and air and improve the efficiency of combustion in a supersonic flow.

Shock waves formed in the combustor duct are reflected from the walls and interact with each other; as a result, a complicated wave structure is formed [28, 29]. The drag force due to skin friction in a supersonic combustor is approximately 30% of the total drag of the vehicle.

It should be noted that acceptable agreement between the calculated and experimental data for external flows does not guarantee that the same numerical methods can be applied for modeling internal flow characterized by the presence of shock waves and expansion waves. Shock waves formed in the combustor duct are reflected from the walls and interact with each other; as a result, a complicated wave structure is formed [28, 29]. The drag force due to skin friction in a supersonic combustor is approximately 30% of the total drag of the vehicle. For determining the flow structure in the channel, which produces an appreciable effect on the combustor parameters, one has to know the pressure field in the entire flow region, as well as the skin friction on the channel walls and the heat flux distribution along the channel [30].

The flows in a channel with a step and a cavity for various Mach numbers were studied in [31, 32] for cold ($T_0 = 300$ K) and high-temperature ($T_0 = 2500$ K) external flows. It was shown that the temperature conditions can significantly affect the separation zone length and the flow structure behind the step. The effect of the temperature factor on the vortex structure formation in the separation zone was considered in those studies. It should be noted, however, that those investigations were performed only for one step configuration.

One of the important factors preventing self-ignition of the hydrogen–air mixture is a high velocity, which is responsible for low static parameters of the mixture. Therefore, it is necessary to study the flow structure, velocity field, and temperature field, and also to determine regions where self-ignition is possible. The physical mechanisms of a supersonic flow in a channel with a backward-facing step is rather complicated and requires further investigations. There is a lack of data on the effects of the Mach number, wall temperature, and degree of flow expansion, especially for high-temperature flows. The step shape, wall temperature, and combustion process are additional factors, which complicate the investigation of the flow in a channel with a step. The effects of these parameters on the combustor flow have to be studied in more detail.

The goal of the present work is to perform a comprehensive experimental and numerical study of the influence of the step configuration on the following parameters: wave structure of the supersonic flow in the channel for the Mach number M = 2.8, positions and sizes of the separation zones on the channel walls, temperature distribution and vortex structure in the flow, ignition of the mixture, and stabilization of combustion of the premixed hydrogen–air mixture.

EXPERIMENTAL INVESTIGATIONS

A channel with a step was tested in a model combustor in the attached pipeline mode in the IT-302M high-enthalpy hotshot wind tunnel [33]. The experimental model is schematically shown in Fig. 1.

The model consists of a settling chamber, replaceable nozzles, insulator section for flow equalization, and working channel for modeling reacting flows in a supersonic combustor. Such a modular principle of model design allows effective utilization of the wind tunnel as a source of a high-enthalpy test gas (air). The set of replaceable contoured nozzles ensures flow regimes with different velocities corresponding to the Mach numbers M = 2.5, 3, 3.5, 4, and 5. The model is equipped with static pressure and heat flux probes on the upper and lower walls of the channel. The side walls of the working channel have (100 × 100)-mm windows made of heat-resistant quartz glass, which allow flow visualization and optical measurements.

The present investigations were performed for the following parameters: Mach number at the combustor entrance $M_\infty = 2.8$, stagnation pressure $p_0 = 3.5$ MPa,

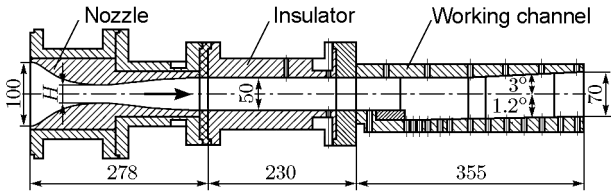

Fig. 1. Experimental facility.

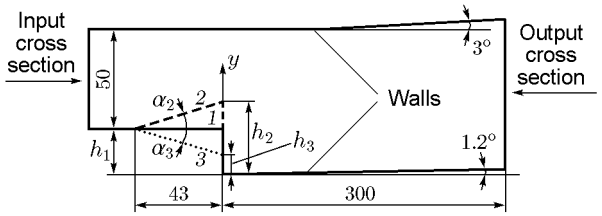

Fig. 2. Computational domain with steps of different configurations: (*1*) straight step with no preliminary action on the flow; (*2*) preliminary compression of the flow; (*3*) preliminary expansion of the flow.

stagnation temperature $T_0 = 1813$ K, static pressure $p_\infty = 0.13$ MPa, and static temperature $T_\infty = 705$ K. As the test time was approximately 100 ms, the model wall remained cold ($T_w = 300$ K), which corresponded to the low value of the temperature factor $k = T_w/T_0 = 0.17$.

The parameters measured in the experiment were the total pressures in the first and second settling chambers of the wind tunnel, flow rates of air and fuel, and static pressure distributions on the model walls. Test preparation included nozzle calibration. The maximum deviation of the Mach number from the nominal value was 1.2%. The root-mean-square deviation of the mean streamwise velocity in the channel varied from 0.5 to 1.5% of the free-stream velocity in different regimes of wind tunnel operation [34]. The velocity fluctuations were 2.5–3%, and the pressure fluctuations were within 5%.

To estimate the parameters of the boundary layer ahead of the combustor, the measurements were performed by a rake consisting of nine Pitot pressure probes. The staggered arrangement of the probes allowed us to minimize the step between the probes and to prevent the mutual influence of shock wave arising around the Pitot probes. One of the probes was mounted in such a way that is contacted the model surface.

MATHEMATICAL MODEL, NUMERICAL ALGORITHM, AND BOUNDARY CONDITIONS

Numerical simulations of the flow in a channel with a backward-facing step were performed in a steady two-dimensional formulation on the basis of Favre-averaged Navier–Stokes equations supplemented with the k–ω SST (shear stress transport) model of turbulence. Application of the two-dimensional approach is based on static pressure measurements in the transverse direction in three cross sections of the model, which showed that the flow remains two-dimensional at least over the width of 75–80% of the model span, and the change in pressure near the wall is within 10%. For calculating reacting flows, the mathematical model was supplemented with species transport equations and Arrhenius-type chemical kinetics including 38 forward and backward reactions of hydrogen–air mixture combustion [35], which revealed good consistency with experimental data on the ignition delay time for hydrogen–air mixtures [36]. The calculations were performed by using the commercial software package ANSYS CFD (Fluent).

Three step configurations were used in the present study (Fig. 2): (1) straight step without preliminary action on the flow; (2) configuration with preliminary compression of the flow; (3) configuration with preliminary expansion of the flow. The computations were performed for the angles $\alpha_1 = \alpha_2 = 8°$ and step heights $h_1 = 16$ mm, $h_2 = 22$ mm, and $h_3 = 10$ mm.

The computational domain of the problem (see Fig. 2) is bounded by the inlet section on the left, by the walls on the top and bottom, and by the outlet section on the right. The computations were performed on a structured grid with quadrangular cells, which was refined toward the solid surfaces. The grid refinement parameter was chosen in such a way that the dimensionless distance from the wall at the first computational node was $y_1^+ \approx 1$ and the laminar sublayer contained approximately ten nodes, which ensured a sufficiently precise resolution of the turbulent boundary layer in the near-wall region and made it possible to perform computations without involving wall functions.

In modeling cold (nonreacting) flows, the channel walls were subjected to the no-slip condition for velocity and the cold wall condition ($T_w = 300$ K) for temperature corresponding to the experimental conditions. The inlet conditions were the profiles of the Mach number, static pressure, and static temperature obtained in preliminary calculations of the flow in a constant-section channel 800 mm long with various initial conditions for turbulence. The results obtained were used for estimating the influence of the wind tunnel turbulence level on the formation of the velocity profile ahead of the step. The predicted skin friction coefficients C_f upstream of the step for the external turbulence levels of 0.5, 1, and 3% are shown in Fig. 3a (curves *1*, *2*, and *3*, respectively). The mean velocity profiles in the coordinates

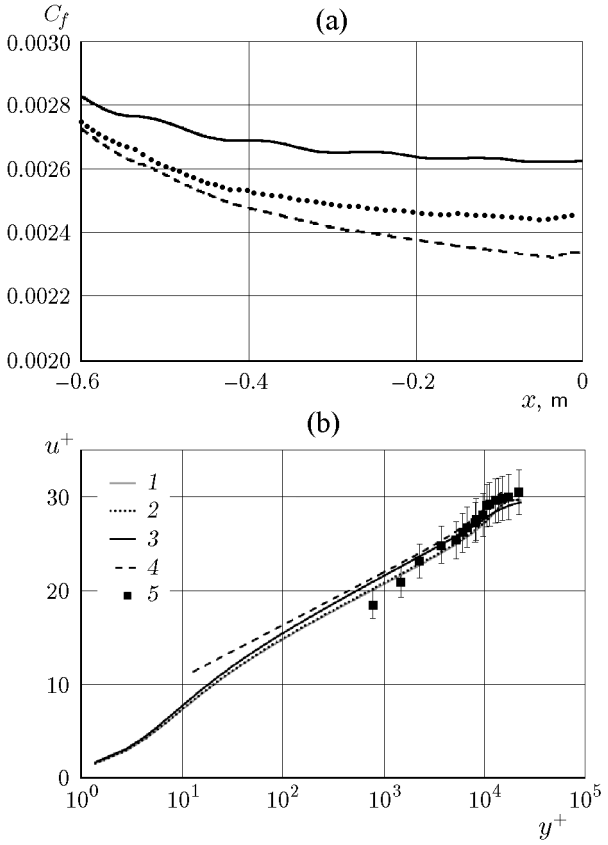

Fig. 3. Distribution of the skin friction coefficient for different turbulence levels (a) and mean velocity profiles upstream of the step in the wall–wake law variables (b): curves *1*, *2*, and *3* show the results for the turbulence levels of 0.5, 1, and 3%, respectively, and curve *4* is based on the wall–wake law; points *5* are the experimental results.

$u^+(y^+)$ are plotted in Fig. 3b, where the wall–wake law [37] (curve *4*) has the form

$$\frac{u^*}{u_\tau} = \frac{1}{\varkappa}\ln y^+ + B + \frac{C}{\varkappa}\left(1 - \cos\frac{\pi y}{\delta}\right)$$

($\varkappa = 0.41$, $B = 5.1$, and $C = 0.58$).

The data obtained show that the predicted curve for the initial turbulence level of 3% almost coincides with the theoretical dependence of the wall–wake law. Some differences in the computed and experimental data are observed only in the near-wall layer, which may be caused by the error of pressure measurements by the Pitot probe near the channel wall and also by the presence of a local separation zone ahead of the probe.

The measurements performed in the study showed that a boundary layer 10 mm thick was formed on the channel walls, which was consistent with the computed data. The outlet section of the computational domain was in the supersonic flow region, except for narrow near-wall regions. The pressure value assigned in the outlet section guaranteed the absence of mass and energy inflow through this cross section. Variations of the outlet section position and flow parameters did not affect the results computed in the upstream region.

Table 1. Computational Grid Parameters

Grid	Number of cells	Step in the y direction, m	
		minimum	maximum
Fine	477 500	$5 \cdot 10^{-6}$	$7 \cdot 10^{-4}$
Medium	272 250	$3 \cdot 10^{-5}$	$1 \cdot 10^{-3}$
Coarse	123 300	$6 \cdot 10^{-5}$	$2 \cdot 10^{-3}$

For studying grid convergence, configuration No. 2 was computed on three different grids whose parameters are summarized in Table 1. A comparison showed that the results obtained on the medium and fine grids differ by less than 1%. Therefore, the medium grid was used in further computations.

RESULTS AND DISCUSSION

Boundary Layer Parameters and Velocity Profiles

Flow pre-compression or pre-expansion ahead of the step alters the integral characteristics of the boundary layer and, correspondingly, the velocity profile ahead of the step. This factor is essential for the flow pattern behind the step; therefore, its influence was analyzed at the first stage of the study.

The integral characteristics of the boundary layer (its thickness δ and displacement thickness δ^*) presented in Table 2 for different temperature conditions reflect the changes in the boundary layer properties depending on the preliminary action type. After interaction of the boundary layer with the compression wave (configuration No. 2), the flow is additionally compressed and the boundary layer thickness decreases. After interaction of the boundary layer with the expansion wave (configuration No. 3), the boundary layer thickness increases. Under the adiabatic wall condition, the boundary layer is thinner for all step configurations.

Wave Structure of the Channel Flow

Figure 4 shows the Mach number fields for three configurations of the step. The flow structure formed in the supersonic flow past the backward-facing step of the basic configuration (Fig. 4a) includes the expansion fan (EF) at the corner point of the step, a recirculation zone (RZ), and a tail shock (TS) in the flow reattach-

Table 2. Boundary Layer Thickness ahead of the Step

Configuration number	T_w = 300 K		Adiabatic wall	
	δ, mm	δ^*, mm	δ, mm	δ^*, mm
1	10.7	2.77	9.04	2.88
2	8.5	2.3	6.9	2.4
3	14.3	4.65	12.3	4.52

ment region. The slope of the first characteristic of the expansion fan is determined by the free-stream Mach number. The slope of the last characteristic and the TS intensity are related to the separation zone size, which, in turn, depends on the free-stream Mach number, initial thickness of the boundary layer, and wall temperature [31]. A local separation zone (SZ) is formed owing to TS interaction with the boundary layer on the upper wall.

In the flow past the step with configuration No. 2 (Fig. 4b), the shock wave *1* formed in the compression corner leads to flow separation on the upper wall (*2*) and then is reflected from the upper wall as a shock wave *3*. The reflected wave is incident onto the wall and leads to boundary layer separation (*4*) and a corresponding increase in static pressure in the region $x = 0.15$ m (Fig. 4b). The repeatedly reflected shock wave *5* merges with the tail shock. As a result, an intense shock wave is formed, which is incident onto the upper wall and forms the separation zone *6*. The large-size SZ reduces the effective cross section of the channel; as a result, the pressure in the channel increases and the Mach number averaged over the cross section decreases.

The flow past the step with configuration No. 3 is accompanied by the formation of a preliminary expansion wave, leading to an increase in the Mach number and a decrease in pressure in the cross section ahead of the step (Fig. 4c). Owing to the change in the wall slope near the step, the angle of flow turning in the expansion corner ($x = 0$) decreases, resulting in significant reduction of the RZ size behind the step. For this reason, the wave structure related to the tail shock is shifted upstream as compared to the basic configuration (No. 1). A comparison of the Mach number flow fields shows that the flow in a channel with a step is decelerated to the greatest extent in the case of flow pre-compression, and the highest velocity is observed for configuration No. 3 with preliminary expansion of the flow.

The experimental Schlieren picture of the flow (Fig. 5) obtained in the high-enthalpy wind tunnel at $M_\infty = 2.8$ and $T_w = 300$ K for the step configuration No. 1 agrees well with the predicted result (see Fig. 4a).

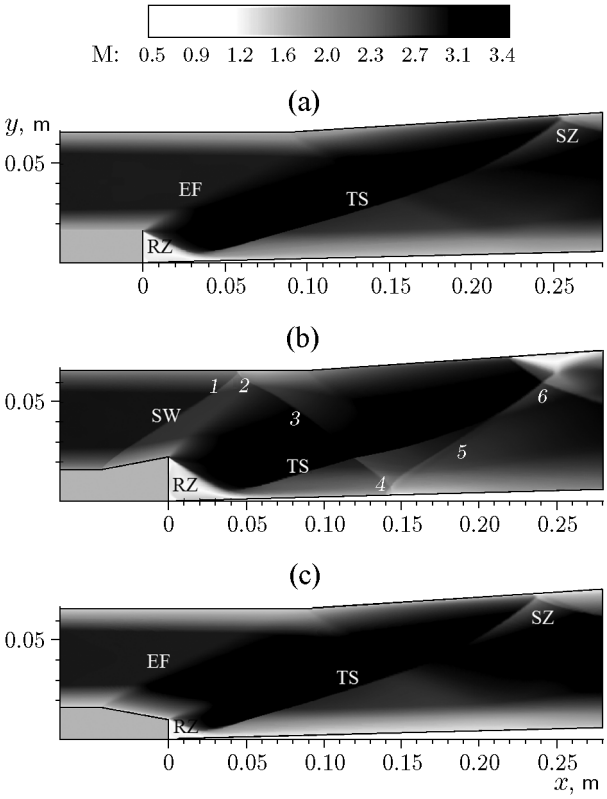

Fig. 4. Computed Mach number fields for the step configuration Nos. 1 (a), 2 (b), and 3 (c): EF is the expansion fan, RZ is the recirculation zone, TS is the tail shock, SZ is the local separation zone, and SW is the shock wave; in Fig. 2b, *1* is the shock wave, *2* is the flow separation on the upper wall, *3* is the reflected shock wave, *4* is the boundary layer separation, *5* is the repeatedly reflected shock wave, and *6* is the separation zone.

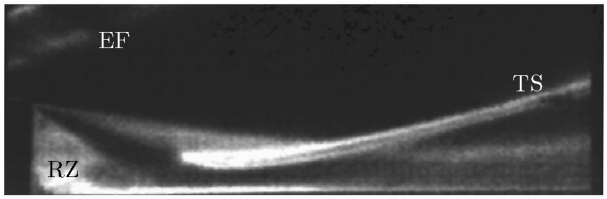

Fig. 5. Experimental schlieren picture of the flow in the channel with the step configuration No. 1.

The quantitative data on the static pressure distributions on the lower and upper walls of the channel and in the core flow are shown in Fig. 6. A comparison of the numerical and experimental data confirms their good quantitative agreement for all step configurations considered. The data in Fig. 6a testify that the base pressure depends on the step configuration. Sudden ex-

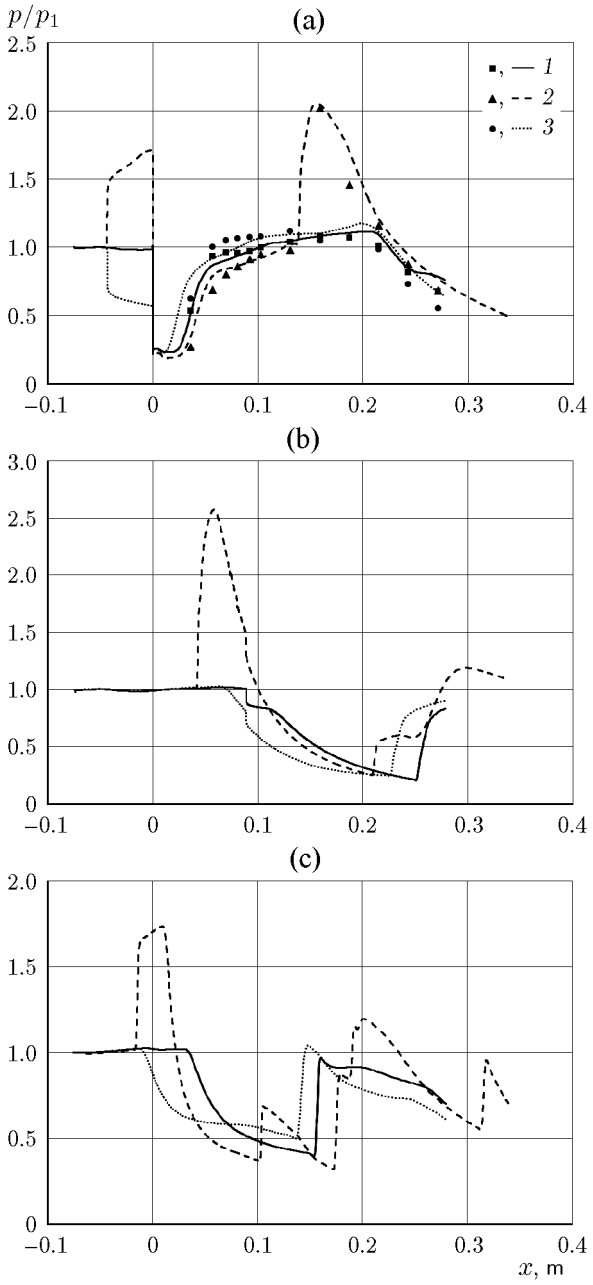

Fig. 6. Static pressure distributions on the lower wall of the channel (a) and upper wall of the channel (b) and in the core flow (c) for the steps with configuration Nos. 1–3 (curves *1–3*, respectively); the points refer to the experimental data.

pansion of the channel leads to a decrease in pressure to a level of 0.2–0.3 of the pressure value ahead of the step. The maximum pressure in the base region was obtained for configuration No. 3, which is consistent with the data for the external flow around constricting rear parts of the vehicles [6, 13]. The use of the step with flow pre-compression (configuration No. 2) leads to a significant increase in the pressure in the channel and to a decrease in the base pressure owing to an increase in the angle of flow turning around the corner point.

Behind the tail shock, the normalized static pressure on the lower wall of the channel is recovered to values close to unity (see Fig. 6a). Further downstream, the pressure behavior is significantly different, depending on the presence or absence of flow pre-compression or pre-expansion.

For configuration Nos. 1 and 3, a monotonic decrease in the pressure on the lower wall at $x > 0.2$ m is observed owing to the action of the expansion fan formed near the step and arriving on the lower wall after reflection from the upper wall of the channel. For configuration No. 2, an appreciable increase in pressure is observed at $x = 0.15$ m, which is due to the incidence of the shock wave *3* (see Fig. 4b), and then the pressure monotonically decreases until the end of the computational domain.

A typical feature of the pressure distribution on the upper wall for configuration No. 2 (Fig. 6b) is the pressure peak caused by the shock wave *1* (see Fig. 4b), formation of a pressure plateau in the separation zone *6*, and further increase in pressure behind the reattachment shock.

It is seen from the static pressure distribution in the core flow (Fig. 6c) that the presence of an additional compression corner leads to the formation of an intense shock wave ahead of the step and significant enhancement of the shock wave closing the separation zone behind the step. As it will be shown below, shock wave enhancement gives rise to large local separation zones on the channel walls.

A change in the step configuration alters the wave structure of the flow; therefore, it is necessary to evaluate the total pressure loss for each step configuration. The total pressure recovery coefficients were calculated as the ratio of the mean total pressure on the inlet and outlet boundaries. The computations predicted the values of the total pressure recovery coefficients equal to 0.794, 0.653, and 0.877 for the step configuration Nos. 1–3, respectively. The maximum total pressure loss is observed for configuration No. 2 because a greater number of shock waves and boundary layer separation zones on the channel walls are formed in this case.

Flow Separation

The data in Table 2 show that the boundary layer parameters ahead of the step can be significantly different, depending on the preliminary action on the flow. Therefore, analyzing the computed results and determining the RZ length, one should take into account the

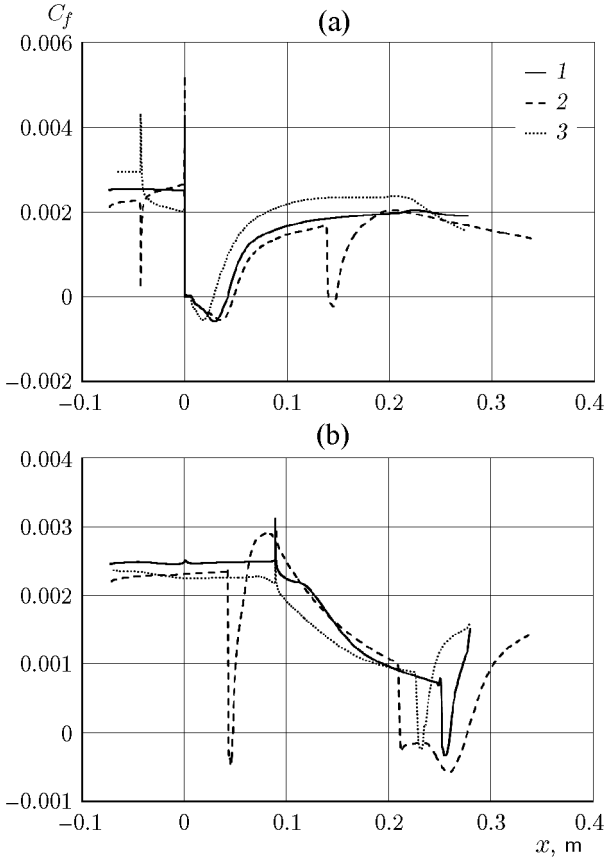

Fig. 7. Computed distributions of the skin friction coefficient on the lower (a) and upper (b) walls of the channel for the steps with configuration Nos. 1–3 (curves *1–3*, respectively).

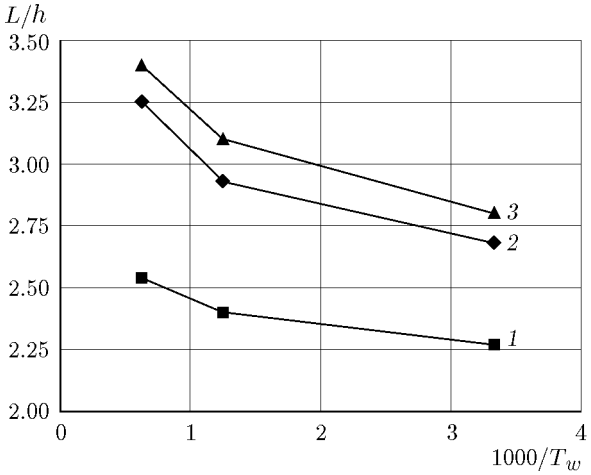

Fig. 8. Normalized separation zone length versus the channel wall temperature for the steps with configuration Nos. 1–3 (curves *1–3*, respectively).

state of the boundary layer in the channel upstream of the channel expansion [3, 4]. The distribution of the skin friction coefficient along the channel walls (Fig. 7) allows one to identify the separation zones on the channel walls as the regions where the friction coefficient takes negative values. The data obtained give grounds to conclude that the minimum length of the separation zone behind the step is provided by using the step with flow pre-expansion (configuration No. 3). The maximum SZ length is obtained for the step with flow precompression (configuration No. 2), which is consistent with the Schlieren visualization results. In this case, separation zones *2* and *6* are formed on the upper wall due to the incidence of the shock waves *1* and *5* (see Fig. 4b), and the separation zone *4* is formed on the lower wall in the region of incidence of the shock wave *3*.

The influence of the wall temperature on the SZ length behind the step was numerically studied earlier in [38, 39] for all step configurations. The computations were performed for cold ($T_w = 300$ and 800 K) and adiabatic temperature conditions on the wall. Figure 8 shows the summary data, which illustrate the changes in the SZ length L normalized to the step height h for each configuration as a function of the wall temperature. The data obtained show that the wall temperature and step configuration are independent factors that affect the SZ length. Reduction of the wall temperature decreases the SZ length for all three step configurations, and the minimum normalized SZ length is observed for configuration No. 2.

Effect of the Flow Temperature

An important characteristic of the flow in the combustor is the flow temperature, which significantly affects self-ignition of the mixture. The analysis performed in [31, 39] revealed the influence of the channel wall temperature on the base pressure, SZ length behind the step, and vortex structure in the separation zone.

The static temperature in the supersonic core flow ahead of the interaction zone is 700 K, and the temperature near the walls increases owing to viscous dissipation. The presence of a low-velocity and, hence, high-temperature recirculation zone behind the step is expected to facilitate ignition. Under adiabatic conditions on the wall, the temperature in the separation zone reaches high values, which are close to the stagnation temperature. However, the cold wall conditions significantly decrease the temperature in the recirculation zone, which may prevent ignition of the mixture [39].

The temperature distribution in the channel is significantly affected by the step configuration. Figure 9 shows the temperature fields and streamlines for different step configurations.

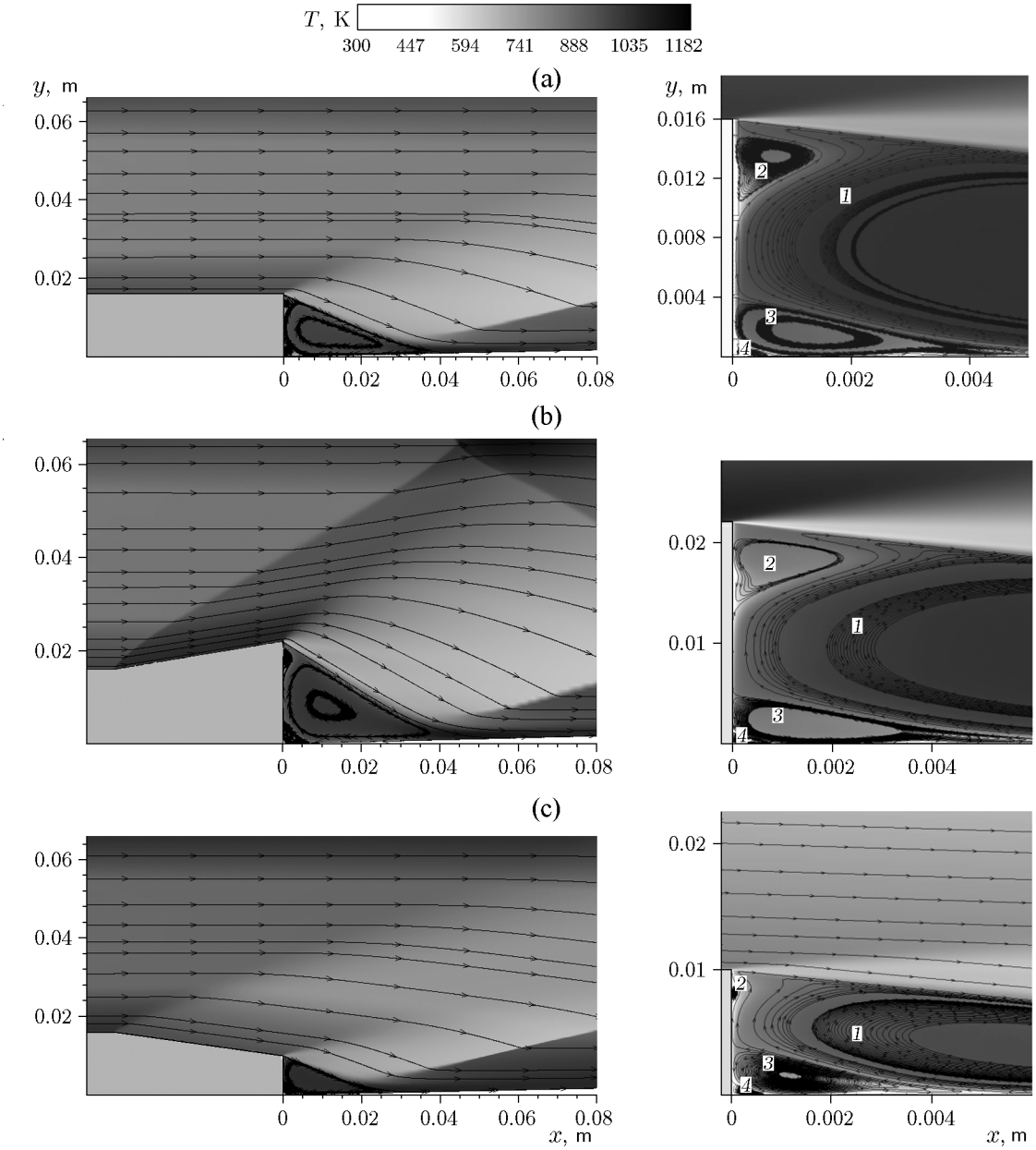

Fig. 9. Static temperature fields and streamlines for the step with configuration Nos. 1 (a), 2 (b), and 3 (c): clockwise-rotating primary vortex for $T \approx 800$ K (*1*), counterclockwise-rotating secondary vortices for $T \approx 650$–700 K (*2* and *3*), and clockwise-rotating secondary vortex for $T \approx 300$ K (*4*).

For configuration No. 1 (Fig. 9a), the static temperature above the separation zone decreases to 400 K because of flow expansion. The maximum temperature of 1100 K is reached at the flow reattachment point $x_R = 43$ mm. A four-vortex structure with a clockwise-rotating primary vortex *1* is formed in the separation zone behind the step; the temperature inside this vortex reaches 800 K. There are also secondary vortices *2* and *3*, which rotate in the counterclockwise direction; the temperature in these vortices is 650–700 K. The magnified image also reveals the existence of a clockwise-rotating secondary vortex *4* with the temperature close to the wall temperature (300 K). The formation of the secondary vortices is caused by the fact that the minimum static pressure is reached at the primary vortex center. When moving from the separation point inward the SZ, the low-velocity near-wall layer passes through the flow region with a negative pressure gradient, which leads to

relaminarization of this layer. Passing under the vortex center, the layer directed toward the vertical face of the step interacts with the flow region with a positive pressure gradient, inducing secondary separation and formation of an additional vortex *3*. A similar situation is observed near the vertical wall. The flow reattached at the face center moves upward, and the static pressure slightly increases. Nevertheless, even this small adverse pressure gradient can separate the low-velocity near-wall layer, resulting in the formation of the vortex *2*.

For the step configuration No. 2 (Fig. 9b), the SZ size increases owing to flow deflection by a greater angle; hence, the size of the external vortex *1* increases. Flow reattachment occurs at $x_R = 50$ mm. An increase in the SZ length leads to an increase in the sizes of the secondary vortices *2–4*. The temperature in the core flow increases to 1100 K behind the shock wave and then decreases to 500 K in the expansion wave.

For the step configuration No. 3 (Fig. 9c), significant reduction of temperature above the separation region typical for configuration Nos. 1 and 2 is not observed because of smoother expansion of the flow. The flow temperature above the mixing layer is approximately 600 K. Flow reattachment occurs at $x_R = 28$ mm. In this case, the minimum RZ length and, correspondingly, the minimum size of the primary vortex *1* are reached. The secondary vortex *2* is formed near the upper edge of the step; the size of this vortex is appreciably smaller than that for two other configurations. The temperature inside the recirculation zone is homogeneous and approximately equal to 800 K.

The quantitative behavior of the temperature in the channel is illustrated in Fig. 10, which shows the static temperature distribution on the line passing through the mid-height of the corresponding step, i.e., at a distance $y = 8$, 11, and 5 mm from the lower wall. The temperature near the vertical face of the step rapidly increases from the values determined by the cold wall conditions (300 K) to sufficiently higher values (900–1000 K) owing to the low velocities of the flow in this region. The temperature decreases again to 500–600 K at the primary vortex center in the separation zone and then drastically increases behind the reattachment shock. After that, the flow pattern qualitatively resembles that described above in analyzing the pressure behavior. The static temperature increases monotonically up to the region where the expansion waves arrive. Configuration No. 2 ensures the greatest SZ length and a drastic increase in temperature in the region of incidence of the shock wave *3* (see Fig. 4b). The lowest temperature at the end of the channel is observed for configuration No. 1.

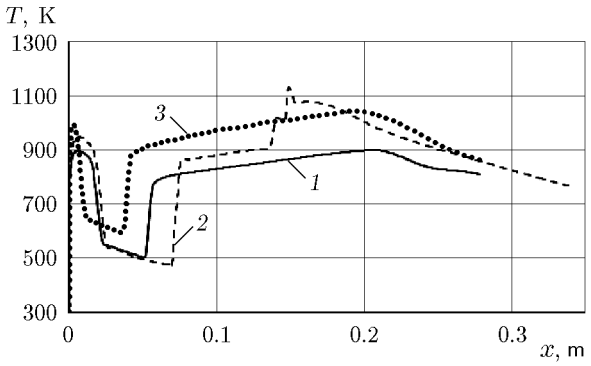

Fig. 10. Calculated temperature distributions along the line passing through the middle of the step with configuration Nos. 1–3 (curves *1–3*, respectively).

Ignition and Flame Stabilization

Numerical simulations of the influence of the step configuration on ignition of the mixture and flame propagation in the channel were performed as a preliminary stage of investigations of the burning flow by an example of ignition of a stoichiometric hydrogen–air mixture. The premixed mixture was chosen to separate the effects of the step shape (flow pre-compression or pre-expansion) and flow structure from the effects of fuel injection and mixing level on ignition and flame stabilization.

The process of ignition of the mixture and flame propagation was calculated for the same flow parameters for which the non-reacting channel flow was previously analyzed; the wall temperature was $T_w = 800$ K, which was close to the wall temperature in a real combustor. The premixed mixture was injected into the combustor in the cross section $x = -0.1$ m ahead of the step.

Figure 11 demonstrates the changes in the calculated normalized static pressure in the channel with the step configuration Nos. 2 and 3 with and without allowance for chemical reactions of hydrogen combustion. It is seen that combustion, which is identified on the basis of the increase in the static pressure above its level in the nonreacting flow, begins immediately behind the region of mixing layer reattachment behind the step. For configuration No. 2, the high value of pressure near the outlet section ($x = 0.28$ m) testifies that the combustion zone extends up to the end of the computational domain.

This is also confirmed by the computed field of the concentration of the reaction product (water) in the channel with the step configuration No. 2 shown in Fig. 12.

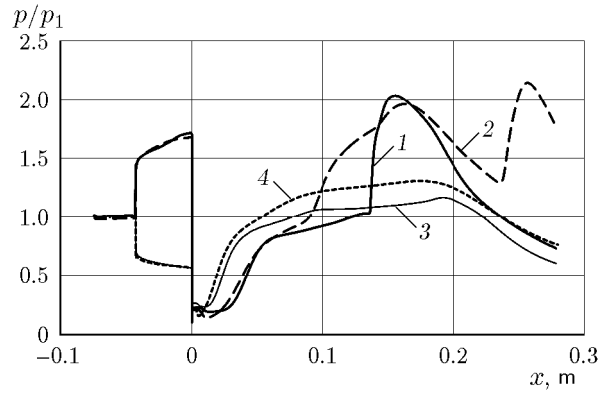

Fig. 11. Static pressure distributions along the lower wall of the channel for the steps with configuration No. 2 (curves *1* and *2*) and No. 3 (curves *3* and *4*) with the chemical reactions of hydrogen combustion being ignored (*1* and *3*) and taken into account (*2* and *4*).

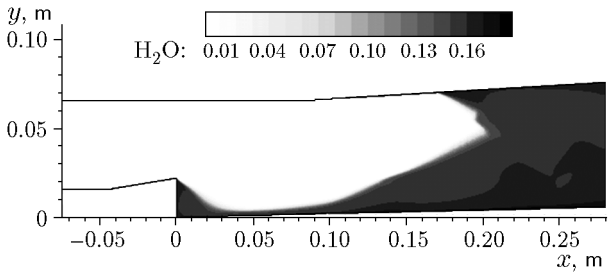

Fig. 12. Calculated field of the mass concentration of water in the channel with the step configuration No. 2.

The combustion zone begins behind the step, which serves as a flame holder. Intense combustion propagates over the entire height of the combustor at a distance of 0.2 m from the step, which is associated with the existence of a vast region of boundary layer separation on the upper wall owing to the action of the shock wave, as described above. It is in the separation zones that the most intense combustion occurs, which is evidenced by the high values of the water concentration.

The use of the step with flow pre-expansion leads to reduction of the heat release intensity, which is confirmed by the static pressure distribution in the channel (curves *3* and *4* in Fig. 11). The increase in pressure begins immediately behind the SZ (behind the step), and it is noticeably smaller than that in the previous case. The increase in pressure in the channel due to combustion does not exceed 30% as compared to the pressure without combustion, whereas the pressure in the case of flow pre-compression increases almost by a factor of 3 (curves *1* and *2* in Fig. 11). The analysis of the calculated fields of the water concentration shows that combustion is not extended over the entire combustor volume: it is confined to the flow region near the lower wall. These changes in the combustion behavior in the channel with flow pre-expansion are caused by the decrease in the step height and the RZ size behind the step. Simultaneously, the flow velocity increases and the density decreases; these are unfavorable factors for mixing and heat release intensification.

As it could be expected, the case without flow pre-compression or pre-expansion occupies an intermediate position, which was confirmed by the calculated result.

CONCLUSIONS

The processes of ignition and flame stabilization for a hydrogen-based fuel in a model combustor at supersonic flow velocities were studied numerically and experimentally. The influence of the configuration of the backward-facing step on the separation zone length, on the wave structure of the flow, and also on the process of ignition in the channel at the Mach number of 2.8 was considered. Based on the present investigations, the following conclusions can be drawn:

- A change in the backward-facing step configuration does not lead to qualitative changes in the vortex structure of the flow behind the step, but the scales of the vortices become different;
- A decrease in the wall temperature (cooling) leads to significant reduction of the separation zone length behind the step;
- The separation zone length depends on the character of the preliminary action on the flow (step configuration); the minimum normalized SZ length is observed for the step configuration with flow pre-compression;
- Flow pre-compression forms the wave structure of the channel flow that increases the static pressure and temperature behind the step and facilitates self-ignition of the hydrogen–air mixture and flame stabilization.

The ignition of the premixed mixture was calculated as a preliminary stage of investigations to separate the effects of the step shape (flow pre-compression or pre-expansion) and flow structure from the effects of fuel injection and mixing level on ignition and flame stabilization. Further calculations will be performed for conditions with distributed injection of the fuel with one of the goals being determination of the influence of the injection scheme on the combustion efficiency.

This work was supported by the Russian Foundation for Basic Research (Grant No. 17-08-01158a).

REFERENCES

1. R. E. Larson and A. R. Hanson, "A Review of Research on Base Flow," AIAA Paper No. 65-825 (1965).
2. I. E. Alber and L. Lees, "Integral Theory for Supersonic Turbulent Base Flow," AIAA J. **6** (7), 1343–1351 (1968).
3. D. C. Reda and R. H. Page, "Supersonic Turbulent Flow Reattachment Downstream of Two-Dimensional Backward Facing Step," AIAA Paper No. 70-108 (1970).
4. J. C. Dutton, J. L. Herrin, M. J. Molezzi, et al., "Recent Progress on High-Speed Separated Base Flows," AIAA Paper No. 95-0472 (1995).
5. H. Liu, B. Wang, Y. Guo, et al., "Research Article Effects of Inflow Mach Number and Step Height on Supersonic Flows over a Backward-Facing Step," Adv. Mech. Eng. **2013** (2013); Article ID 147916; http://dx.doi.org/10.1155/2013/147916.
6. J. L. Herrin and J. C. Dutton, "Supersonic Near-Wake Afterbody Boattailing Effects on Axisymmetric Bodies," J. Spacecraft Rockets **31** (6), 1021–1028 (1994).
7. B. F. Armaly, F. Durst, J. C. F. Pereira, and B. Schoenung, "Experimental and Theoretical Investigation of Backward Facing Step Flow," J. Fluid Mech. **127**, 473–496 (1983).
8. S. Thangam and D. D. Knight, "Effect of Step Height on the Separated Flow past a Backward Facing Step," Phys. Fluids. A **1** (3), 604–615 (1989).
9. F. Scarano, C. Benocci, and M. L. Riethmuller, "Pattern Recognition Analysis of the Turbulent Flow Past a Backward Facing Step," Phys. Fluids **11** (12), 3808–3818 (1999).
10. L. Rollstin, "Measurement of Inflight Base Pressure on an Artillery Fired Projectile," AIAA Paper No. 87-2427 (1987).
11. R. Deepak, S. L. Gai, ad A. J. Neely, "A Computational Study of High Enthalpy Flow over a Rearward Facing Step," AIAA Paper No. 2010-444 (2010).
12. V. Statnikov, D. Saile, J.-H. Mei, et al., "Experimental and Numerical Investigation of the Turbulent Wake Flow of a Generic Space Launcher Configuration," Prog. Flight Phys. **7**, 329–350 (2015).
13. J. Parker-Lamb and W. L. Oberkampf, "Review and Development of Base Pressure and Base Heating Correlations in Supersonic Flow," J. Spacecraft Rockets **32** (1), 8–23 (1995).
14. M. K. Aukin and R. K Tagirov, "Calculation of the Base Pressure and Enthalpy behind a Plane or Axisymmetric Step in a Supersonic Flow with due Allowance for the Influence of the Initial Boundary Layer," Izv. Ross. Akad. Nauk, Mekh. Zhidk. Gaza, No. 2, 110–119 (1999).
15. T. Mathur and J. C. Dutton, "Velocity and Turbulence Measurements in a Supersonic Base Flow with Mass Bleed," AIAA J. **34** (6), 1153–1159 (1996).
16. D. R. Smith and A. J. Smits, "The Rapid Expansion of a Turbulent Boundary Layer in a Supersonic Flow," J. Theor. Comput. Fluid Dyn. **2** (5/6), 319–328 (1991).
17. S. A. Arnette, M. Samimy, and G. S. Elliott, "The Effect of Expansion on the Large Scale Structure of a Compressible Turbulent Boundary Layer," AIAA Paper No. 93-2991 (1993).
18. S. M. Correa and R. E. Warren, "Supersonic Sudden-Expansion Flow with Fluid Injection: an Experimental and Computational Study," AIAA Paper No. 89-0389 (1989).
19. A. S. Yang, W. H. Hsieh, and K. K. Kuo, "Theoretical Study of Supersonic Flow Separation over a Rearward-Facing Step," J. Propul. Power **13** (2), 324–326 (1997).
20. P. Manna and D. Chakraborty, "Numerical Investigation of Transverse Sonic Injection in a Non-Reacting Supersonic Combustor," J. Aerospace Eng. **219** (3), 205–216 (2005).
21. K. M. Smith and J. C. Dutton, "Investigation of Large-Scale Structures in Supersonic Planar Base Flows," AIAA J. **34** (6), 1146–1152 (1996).
22. B. Sainte-Rose, N. Bertier, S. Deck, and F. Dupoirieux, "A DES Method Applied to a Backward Facing Step Reactive Flow," C. R. Akad. Sci., Ser. IIB: Mecanique **337**, 340–351 (2009).
23. A. Karimi, S. D. Wijeyakulasurya, and M. Razi Nalim, "Numerical Study of Supersonic Flow over Backward-Facing Step for Scramjet Application," AIAA Paper No. 2012-4001 (2012).
24. J. D. Abbitt III, C. Segal, J. C. McDaniel, et al., "Experimental Supersonic Hydrogen Combustion Employing Staged Injection behind a Rearward-Facing Step," J. Propul. Power **9** (3), 472–478 (1993).
25. S. Takahashi, G. Yamano, K. Wakai, et al., "Self-Ignition and Transition to Flame-Holding in a Rectangular Scramjet Combustor with a Backward Step," Proc. Combust. Inst. **28** (1), 705–712 (2000).
26. C. Morrison, H.-Y. Lyu, and R. Edelman, "Fuel Sensitivity Studies Based on a Design System for High Speed Airbreathing Combustors," ISABE 99-7235 (1999).
27. W. Huang, M. Pourkashanian, L. Ma, et al. "Investigation on the Flameholding Mechanisms in Supersonic Flows: Backward-Facing Step and Cavity Flameholder," J. Visualization **14** (1), 63–74 (2011).

28. K. Uenishi, R. C. Rogers, and G. B. Northam, "Numerical Predictions of a Rearward-Facing-Step Flow in a Supersonic Combustor," J. Propul. Power **5** (2), 158–167 (1988).
29. F. H. Tsau and W. C. Strahle, "Prediction of Turbulent Combustion Flowfields behind a Backward-Facing Step," J. Propul. Power **6** (3), 227–236 (1990).
30. M. G. Owens, S. Tehranian, C. Segal, and V. A. Vinogradov, "Flame-Holding Configurations for Kerosene Combustion in a Mach 1.8 Airflow," J. Propul. Power **14** (4), 456–461 (1998).
31. I. A. Bedarev, M. A. Goldfeld, Yu. B. Zakharova, and N. N. Fedorova, "Investigation of Temperature Fields in Supersonic Flow behind a Backward-Facing Step," Teplofiz. Aeromekh. **16** (3), 375–386 (2009) [Thermophys. Aeromech. **16** (3), 355–366 (2009)].
32. M. A. Goldfeld, Yu. B. Zakharova, and N. N. Fedorova, "A Numerical and Experimental Study of the High-Enthalpy High-Speed Cavity Flow," Teplofiz. Aeromekh. **19** (6), 673–687 (2012) [Thermophys. Aeromech. **19** (6), 541–554 (2012)].
33. L. N. Puzyrev and M. I. Yaroslavtsev, "Stabilization of Gas Parameters in the Settling Chamber of a Hypersonic Hotshot Wind Tunnel," Izv. Sib. Otd. Akad. Nauk SSSR, No. 5, 135–140 (1990).
34. Yu. V. Gromyko, A. A. Maslov, A. A. Sidorenko, et al., "Calculation of Flow Parameters in Hypersonic Wind Tunnels," Vestnik Novosib. Gos. Univ., Ser. Fiz. **6** (2), 10–16 (2011).
35. J. H. Tien and R. J. Stalker, "Release of Chemical Energy by Combustion in a Supersonic Mixing Layer of Hydrogen and Air," Combust. Flame **130**, 329–348 (2002).
36. I. A. Bedarev and A. V. Fedorov, "Comparative Analysis of Three Mathematical Models of Hydrogen Ignition," Fiz. Goreniya Vzryva **42** (1), 26–33 (2006) [Combust., Expl., Shock Waves **42** (1), 19–26 (2006)].
37. Tuncer Cebeci, *Analysis of Turbulent Flow* (Elsevier, 2004).
38. N. N. Fedorova, I. A. Bedarev, Y. V. Zhakharova, and M. A. Goldfeld, "Step Configuration Influence on Combustion in Premixed Hydrogen–Air Supersonic Flow," in *ECCOMAS 2012—European Congress on Computational Methods in Applied Sciences and Engineering: E-Book Full Papers* (2012), pp. 6074–6088.
39. M. A. Goldfeld, N. N. Fedorova, and Yu. V. Zakharova, "Influence of Step Configuration on Supersonic Turbulent Flow in Base Region," in *Proc. of 51st Israel Annu. Conf. on Aerospace Sciences, Tel Aviv–Haifa, Israel, February 23–24, 2011.*